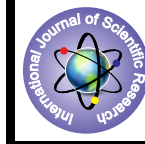


## Impact of Heat treatment on some physical properties of thin CdZnS Films



### Physics

**KEYWORDS:** CdZnS films, Structural properties, Optical and electrical properties, Annealing effect.

<b>Iqbal S.Naji</b>	Physics Department, Science College, University of Baghdad, p.O.Box 47162 , Jadiriya, Baghdad, Iraq
<b>M.F.A.Alias</b>	Physics Department, Science College, University of Baghdad, p.O.Box 47162 , Jadiriya, Baghdad, Iraq
<b>Eman M. Naser</b>	Physics Department, Science College, University of Baghdad, p.O.Box 47162 , Jadiriya, Baghdad, Iraq

### ABSTRACT

Cadmium Zinc Sulfide (CdZnS) thin films have been deposited from their two binary compound CdS and ZnS by vacuum co-evaporation technique. The Structure, optical, and electrical properties of these films which deposited on heated glass substrate at 423 K under vacuum  $10^{-5}$  mbar with thickness 500nm and deposition rate 0.833 nm/sec, and treated at different annealing temperatures were carried out. X-ray diffraction analysis showed polycrystalline nature and have the hexagonal structure with strong preferential orientation along the (002) planes. The optical measurement showed the CdZnS films have direct energy gap ( $E_g$ ), and its varies from 3.1 eV for as deposited to 3.4 eV for annealed film at 473 K. The electrical conductivity decrease many order when these films annealed at different annealing temperature.

### 1. Introduction:

Band gap energy is one of the most important parameters that characterize a semiconductor and determines many gross electronic and optical properties. II-VI semiconductors with energy gaps covering the visible spectral range are compatible candidates for optoelectronic devices[1].

Cadmium sulfide (CdS) , an n-type direct gap semiconductor with room temperature band gap energy of 2.42 eV, has been found to be best suited for thin film CdTe and CuInSe<sub>2</sub> solar cells. However, the band gap energy of CdS is relatively small for CdS/CdTe heterojunction solar cells, since 0.1 $\mu$ m of a CdS film absorbs 36% of the incident radiation with energy higher than 2.42 eV. The band-gap energy of CdS can be increased by the addition of zinc sulfide (ZnS,  $E_g=3.66$  eV)[2], the replacements of CdS with higher band gap CdZnS alloys has led to a decrease in window absorption loss, and has resulted in an increase in the short circuit current in the solar cell [3]and decrease of lattice mismatching with CuInGaSe chalcopyrite semiconductors[4].

CdZnS alloy compounds have attracted technological interest because the energy gap can be tuned and the lattice parameters can be varied [5]. In recent years the replacement of CdS with its ternary alloy CdZnS has been attempted for improvement of the CdZnS/CuInGaSe<sub>2</sub> solar cell performance [6].

The information available on ternary CdZnS system is very limited. It is well established that CdZnS film possess properties between those of ZnS and CdS. Since their addition produces a common lattice in which band structure has a larger band gap than CdS. Thin film studies of ZnS & CdS type materials are very important because of their wide technological applications e.g. ACTFEL panels, flat TV screen, sensitive photoconductor, IR detector, solar cell, and light emitting devices [7].

The CdZnS films has been prepared by various method such as vacuum evaporation [8,9], spray pyrolysis [10-13], chemical bath deposition [14-16], chemical vapor deposition method assisted with laser ablation [1], screen-printing [17,18]. In this work, CdZnS thin films have been prepared by using co-evaporation of CdS and ZnS from two horizontal source. The structural, optical, and electrical properties have been investigated as a function of annealing temperature.

### 2. Experimental Details:

CdZnS thin films of thickness 500nm were prepared from two powder source Cadmium sulfide and Zinc sulfide (5N purity) by using co-evaporation technique in  $10^{-5}$  mbar vacuum from two resistive molybdenum crucible onto ultrasonically clean glass substrate heated to 423 K. The deposition rate fixed at 0.833

nm/sec. A post deposition annealing was performed in air at (373, 423, 473 K) for half an hour.

The structure of prepared CdZnS films was studied by using X-ray diffraction analysis, model Shimadzu-6000 with a  $\text{CuK}\alpha$  x-ray source in range 20 $^\circ$ -60 $^\circ$  of  $2\theta$ . The morphology of prepared thin films was examined by using atomic force microscopy (AFM).

Transmittance (T) and absorbance (A) spectra of the prepared samples were measured by normal incidence of light using spectrophotometer model (UV/VIS sp-3000 plus) in wavelength range 400-1100 nm, using a blank substrate as reference position.

The electrical properties measurements include d.c conductivity and Hall Effect were performed by deposited Aluminum electrodes on these films.

The electrical conductivity measured over the temperature range 303-513 K through digital electrometer Keithley (616) and d.c power supply type (PE-1540). The Hall coefficient (RH), concentration (n) and mobility ( $\mu$ ) of the carrier have been determined from Hall Effect measurement by using the following equations respectively.

$$R_H = \frac{V_H \cdot t}{I \cdot B} \dots\dots\dots(1)$$

$$n = \frac{1}{e \cdot R_H} \dots\dots\dots(2)$$

$$\mu_H = \frac{\sigma}{e \cdot n} \dots\dots\dots(3)$$

Where I represent the current through the sample, B magnetic induction and t thickness of the samples, which carried out by using Hall effect measurement system (3000 HMS) at room temperature.

### 3. Results and discussion:

#### 3-1. Structural Properties

Figures (1) displays XRD patterns for as deposited CdZnS film and annealed at 473 K.

It is observed that the diffraction patterns show polycrystalline nature and exhibited sharp peaks at  $2\theta$  equal to 25.6 $^\circ$ , 26.6 $^\circ$ , 28.7 $^\circ$ , and 47.9 $^\circ$  which correspond to reflections from (100),(002),(101) and (103) planes of hexagonal phase respectively.

The peaks position are in good agreement with JCPDS card data (40-834) for hexagonal CdZnS of peak position 25.50°,26.667°,28.77°, and 48.15°.

The XRD pattern reveals that the (002) reflection is the most intensive in hexagonal phase, which indicates a general tendency that the c-axis of the CdZnS is preferentially perpendicular to the thin film surface.

Same result have been found by Kumar et. al.[3], and Jae et. al.[2].Also Wongcharonen and Gaewdang [4]found the Cd<sub>1-x</sub>Zn<sub>x</sub>S films with atomic fraction x<0.9 is belong to hexagonal wurtzite structure with a preferential orientation (002) plane.

There is no diffraction peaks associated with CdS and ZnS phases. Xia et al. [5] also observed the absence of CdS and ZnS peaks which means the film have single phase.

The diffraction patterns of the film that deposited at 423 K and annealed at 473 K showed sharp peaks at 2θ equal to 25.72°,26.68°,28.85°, and 48.03° as shown in figure (1 b). The height of the (002) peak increased for annealing films this attributed to increase in grain size, where the grain size increase from 30.7 nm to 31.6 nm when film annealed.

It was observed that the diffraction angle of (002) for CdZnS films shifted towards higher angles with an increase annealing CdZnS films, which means that the (002) lattice constant decreases(the c value decrease from 6.692 for as deposited film to 6.676 for annealed film).

Table (1) shows the values of bragg's angles, interplaner spacing, relative intensity and miller indices of CdZnS films.

Sample	2θ <sub>Exp.</sub> (deg.)	2θ <sub>Stan.</sub> (deg.)	d(A°)	I/I <sub>o</sub>	hkl
As deposited	25.69	25.50	3.463	10	100
	26.61	26.66	3.346	100	002
	28.77	28.77	3.100	32	101
	47.97	48.15	1.894	6	103
Annealing at 473K	25.72	25.50	3.460	5	100
	26.68	26.66	3.338	100	002
	28.85	28.77	3.091	20	101
	48.03	48.15	1.892	3	103

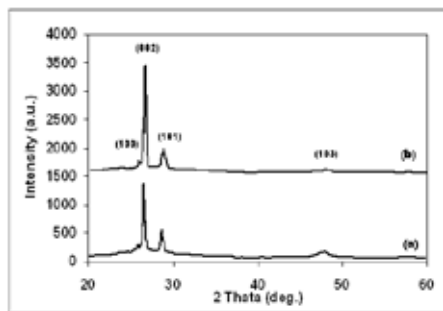


Fig.( 1) x-ray diffraction pattern of CdZnS thin films, a- as deposited b- annealed at 473 K.

3-2. Morphological properties

Typical surface morphologies of as deposited CdZnS films and annealed at 473K in two and three dimensional are shown in Fig. (2). It's observed from the AFM micrograph confirms that the grains are uniformly distributed within the scanning area (1600nm x 1600nm). An initial visual investigation of the de-

posited film as grown and annealed at 473K has shown that they are compact and have good adherence to the substrate. Also the three-dimensional AFM images show that both films are polycrystalline and homogenous, the thin films were composed of multilayered grains. Also we can notice that the grains are in nano-size and nanostructure range. The values of grain size increases with increasing of annealing temperature. The values of the average grain size variable from 70.23 to 91.61nm for as grown and annealed films at 473K respectively. It is observed from Table(2) that the RMS roughness value increases after annealing at 473K. This result indicates that the growth of larger grains with increasing temperature leads to an increase in the surface roughness.

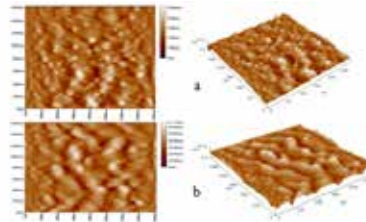


Fig.(2) AFM images of thin CdZnS films (a) as grown at room temperatures, (b) annealed at 473K.

Table (2) The grain size and roughness for as grown and annealed CdZnS films

T <sub>a</sub>	RMS roughness(nm)	Grain size (nm)
as grown	0.866	70.23
473K	5.790	91.61

3-3. Optical properties

The study of optical absorption has proved to be very useful for elucidation of the electronic structure of these materials. It is possible to determine indirect and direct transition occurring in band gap of the materials by optical absorption spectra. The data transmittance can be analyzed to determine optical constants such as refractive index (n), extinction coefficient (k) and dielectric constant (ε). The evaluation of refractive indices of optical materials is of considerable importance for applications in integrated optic devices such as switches, filters and modulators, etc., where the refractive index of a material is the key parameter for device design.

a- Optical Band Gap

In order to determine the optical band gap of CdZnS films, the absorbance spectra of the films were recorded at room temperature in the range of wavelength 200-1100 nm. Also the transmission spectra of as deposited and annealed films were measured as shown in fig.(3).Optical transmission spectra of CdZnS films on glass showed the usual interference pattern of a high index film in the range of low absorption with a sharp fall of transmittance at the band edge, which was an indication of the good crystallinity of the film. The absorption edges of the films were observed to shift towards shorter wavelength with respect to the increasing annealing temperature. This figure shows that the as deposited film have a higher transmittance as compared with other films which annealed at (373,423,and 473)K. This means the untreated films is the best for window applications. Figure (4) shows the absorption coefficient versus the wavelength. It is clear that the absorption coefficient have a high value ( <math>\le 10^4</math>) which means the material have direct band gap. There is blue shift in the absorption edge, it is a reflection of increase in band gap, resulting from the effect of annealing temperature. Asogwa [19] found that with increasing annealing temperature, the optical edge shifts towards the lesser value of wavelength.

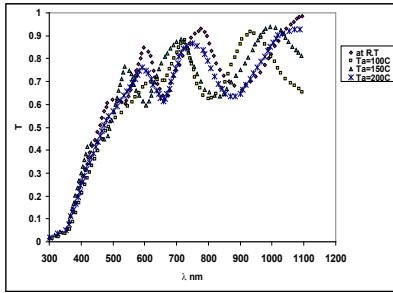


Fig. (3) Transmittance vs. wavelength for CdZnS films at room temperature and different annealing temperatures.

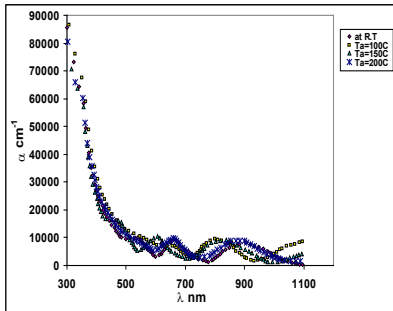


Fig. (4) Absorption coefficient vs. wavelength for CdZnS films at room temperature and different annealing temperatures.

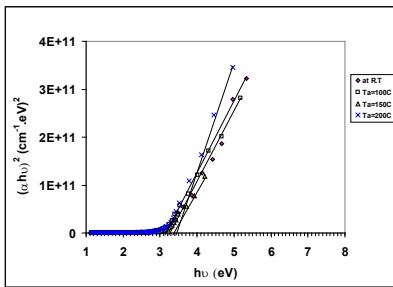


Fig. (5)  $(\alpha h\nu)^2$  vs.  $(h\nu)$  plots for thin CdZnS films

The optical band gap can be calculated from equation (1). Figure (5) shows plots of  $(\alpha h\nu)^2$  versus photon energy  $(h\nu)$  for thin CdZnS films. Linearity of the plots indicates that the material is of direct band gap nature. The extrapolation of the straight line to  $(\alpha h\nu)^2 = 0$  axis gives the energy band gap of the film material. The values of the direct band gap ( $E_g$ ) were determined and given in Table (3).  $E_g$  values change with the annealing temperatures. The optical energy gap was found to increase with the increase of the thermal annealing temperature. It was increased from 3.1 eV for an annealed film to 3.4 eV for film annealed at 473 K. This result of as deposited film is agreement with result shown by Lee et. al.[2]and Kumar et. al. [3] who found that the energy gap of CdZnS films equal to 3.0eV and 3.12eV respectively. The energy gap broadening in the annealing films may be related to the existence with in the band gap of a high density of levels with energies near the bands which can give rise to band tailing, as has been suggested for other polycrystalline materials. The increase in the optical energy gap may be due to the increase in the particle size which leads to decrease the defect stats.

**b-Optical Constants**

The variation of refractive index (n) with wavelength for as deposited and annealed films at different annealing temperature (373,423,473)K are given in figure (6). From this figure we observed that the refractive index decrease with the increase of wavelength of the incident photon. At wavelength equal to 360 nm the refractive index increased from 2.323 for as deposited film to 2.533 for film annealed at 473 K. Kumer et al. [8] found the refractive index value equal to 2.464 at 500 nm wavelength for Cd<sub>0.4</sub>Zn<sub>0.6</sub>S films.

Table(3) the optical constants of CdZnS thin films at different annealing temperatures.

$\lambda=360$ nm						
$T_a$ (K)	$E_g^{opt}$ (eV)	$\alpha$ (cm <sup>-1</sup> ) * 10 <sup>4</sup>	n	k	$\epsilon_r$	$\epsilon_i$
as deposited	3.10	4.956	2.323	0.143	5.376	0.664
373	3.25	5.888	3.60	0.170	13.670	1.265
423	3.30	4.831	2.173	0.138	4.702	0.603
473	3.40	5.124	2.533	0.147	6.395	0.746

3.4 eV for film annealed at 473 K. This result of as deposited film is agreement with result shown by Lee et. al.[2]and Kumar et. al. [3] who found that the energy gap of CdZnS films equal to 3.0eV and 3.12eV respectively. The energy gap broadening in the annealing films may be related to the existence with in the band gap of a high density of levels with energies near the bands which can give rise to band tailing, as has been suggested for other polycrystalline materials. The increase in the optical energy gap may be due to the increase in the particle size which leads to decrease the defect stats

The increase in the refractive index with increasing the annealing temperature for CdZnS thin films is attributed to improvement the (002) hexagonal phase when we annealed these films and this leads to increase the packing density.

Figure (7) shows the variation of extinction coefficient (k) with the wavelength for as deposited and annealed CdZnS films. It is clear that the extinction coefficient increase from 0.143 to 0.147 for as deposited and annealed film at 473 K respectively, at wavelength equal to 360 nm.

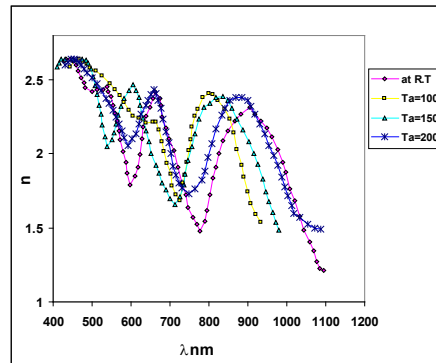


Fig. (6) The refractive index vs. the wavelength for CdZnS films at room temperature and different annealing temperatures

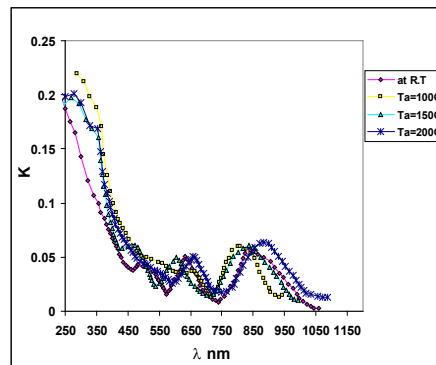


Fig. (7) The extinction coefficient vs. the wavelength for CdZnS film at room temperature and different annealing temperatures.

Figures (8) and (9) show the effect of thermal annealing on the real ( $\epsilon_r$ ) and imaginary ( $\epsilon_i$ ) parts of the dielectric constant for as deposited CdZnS thin films of thickness 500 nm.

The behavior of the  $\epsilon_r$  and  $\epsilon_i$  with annealing temperatures is the same as that of  $n$  and  $k$  respectively.

At wavelength equals to 360 nm the real part of dielectric constant increased from 5.376 for as deposited film to 6.395 for film annealed at 473 K.

The imaginary part increased from 0.664 for un annealed film to 0.746 for film annealed at 473 K at wavelength equal to 360 nm.

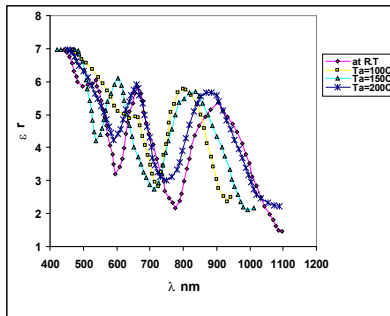


Fig. (8)  $\epsilon_r$  vs. the wavelength for CdZnS films at room temperature and different annealing temperatures.

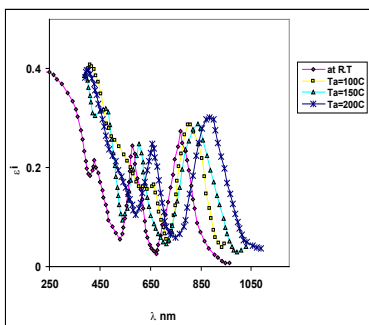


Fig. (9)  $\epsilon_i$  vs. the wavelength for CdZnS films at room temperature and different annealing temperatures.

### 3-4 Electrical Properties

In order to study conductivity mechanisms, it is convenient to plot logarithm of the conductivity ( $\ln \sigma$ ) as a function of  $1000/T$  for CdZnS films in the range (303 – 513) K, as shown in Fig. (10).

It is clear from this Figure that there are two transport mechanisms giving rise to two activation energies  $E_{a1}$  and  $E_{a2}$ .

The conductivity and the activation energies are illustrated in Table (4). It is clear that the conductivity decrease with heat treatment of the film at different annealing temperatures, while the activation energies increase.

An increase in the resistivity with increasing annealing temperatures could be due to an increase in the band gap of CdZnS thin films.

The type of charge carriers, carrier concentration ( $n_H$ ) and Hall mobility ( $\mu_H$ ) of charge carries have been estimated from Hall measurements. It is obvious from the negative sign of the Hall coefficient the type of carrier is donor (n-type charge carries). Table (4) shows the Hall parameters for as deposited CdZnS film and film treated at different annealing temperatures.

It can be observed from this table that the carriers concentration increase while the mobility decrease with increasing of annealing temperatures. The decrement in Hall mobility attributed to the increase of stacking fault density and miss orientation of the crystallites[18].

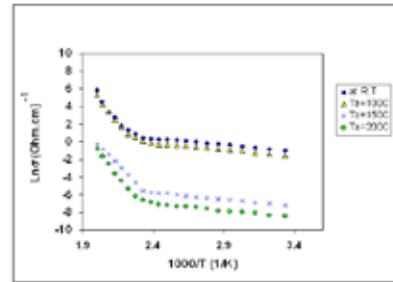


Figure (10)  $\ln \sigma$  versus  $1000/T$  for CdZnS films.

**Table (4): The electrical measurements of CdZnS thin films treated at different annealing temperatures.**

$T_a$ (K)	$\sigma_{RT} \times 10^{-2}$ ( $\Omega \cdot \text{cm}$ ) <sup>-1</sup>	$E_{a1}$ (eV)	$E_{a2}$ (eV)	$n_H \times 10^{18}$ ( $\text{cm}^{-3}$ )	$\mu_H \times 10^{-2}$ ( $\text{cm}^2/\text{V} \cdot \text{s}$ )
as deposited	36.78	1.361	0.1199	0.226	1017
373	20.18	1.373	0.1283	5.62	22.44
423	0.074	1.3956	0.1309	8.17	0.057
473	0.022	1.5975	0.1382	22.48	0.0062

### 4. Conclusions:

CdZnS thin films have been deposited by vacuum co-evaporation method on glass substrates at temperature 473K, and treated at different annealing temperatures. The structure of films was analyzed by x-ray diffraction and the results obtained showed that the films structure is polycrystalline and have hexagonal structure. The measurements of optical transmittance for CdZnS films demonstrate a high transmission values in the wavelength range, and there is a blue shift in the absorption edge. The optical absorption spectra of the films showed that the absorption mechanism is due to direct transitions, and the optical energy gap increase with increasing annealing temperature. The electrical conductivity decrease with the increase of annealing temperature. However, as deposited CdZnS films without any heating treatment is considered as the best of all these films because of its higher conductivity and very low absorption in the visible rang which is suitable to use as a window material in heterojunction solar cells.

### REFERENCE

1- R. Venugopal, P. Lin, and Y. Chen, J.Phys. Chem. B, 110(2006)11691-11696. 2- J.Lee, W. Song, J. Yi, K. Yang, W. Han, J. Hwong, Thin solid films, 431-432(2003) 349-353. 3- T. P. Kumar, K.S. Anan, Chalcogenide Letters, 6(10)(2009)555-562. 4- G.Jia, N.Wang, L.Gong, X.Fei, Chalcogenide Letters, 7(5)(2010)349-355. 5- D.Xia, T. Caijuan, T.Rongzhe, L.We, F.Lianghnan, Z. Jingquans, W. Lili, and L. Zhi, Journal of Semiconductors, 32(2)(2011)1-4. 6- N.Gaewdang, T.Gaewdang and W. Lipar, Technical Digest of the International PVSEC-14,2004. 7- Ayush Khare, Chalcogenide Letters, 6(12)(2009)661-671. 8- P.Kumar, P.N.Dixit, and T.P.Sharma, Indian Journal of engineering & materials sciences, 14(2007)313-316. 9- J.H.Lee, W.Song, J.S.yi, Y.S.Yoo, Solar energy materials & Solar cells, 75(2003)227-234. 10- M.Bedir, R.Kayali, and M.Oztas, Turk J,phys., 26(2002)121-126. 11- S.Ilican, Y.Caglar and M.Caglar, Physica Macedonica, 56(2006)43-48. 12- P.Raji, K.Ramachandran, C.Sanjeeviraja, J.Mater. Sci.,41(2006)5907-5914. 13- S.Ilican, Y.Caglar and M.Caglar, J.of optoelectronics and advanced materials, 9(5)(2007)1414-1417. 14- T.P.Kumar, K.S.Anan, Chalcogenide letters, 6(11)(2009)617-622. 15- V.B.Sanap, B.H.Pawar, Journal of optoelectronics and Biomedical Materials, 3(2)(2011)39-43. 16- I.A.Ezenwa, A.J.Ekpunobi, Journal of Non-oxide glasses,3(3)(2011)77-87. 17- A.M.Patil, and L.A.Patil, Trends in Applied Sciences Research, 1(6)(2006)645-649. 18- D.Patidar, N.S.Saxena, K.Sharma, T.P.Sharma, Optoelectronics and advanced materials- Rapid communications, 1(7)(2007)329-332. 19- P.U.Asogwa, Chalcogenide letters, 7(8)(2010)501-508.